Available online at www.sciencedirect.com

SCIENCE DIRECT

Thin Solid Films 474 (2005) 64–69

www.elsevier.com/locate/tsf

Electrodeposition of polypyrrole/multiwalled carbon nanotube composite films

Gaoyi Han[a,b], Jinying Yuan[a], Gaoquan Shi[a,*], Fei Wei[c,*]

[a]*Department of Chemistry, Tsinghua University, Beijing 100084, PR China*
[b]*Institute of Molecular Science, Chemical Biology and Molecular Engineering Laboratory, Education Ministry, Shanxi University, Taiyuan 030006, PR China*
[c]*Department of Chemical Engineering, Tsinghua University, Beijing 100084, PR China*

Received 14 January 2004; received in revised form 16 July 2004; accepted 9 August 2004
Available online 29 September 2004

Abstract

The nanocomposite films of polypyrrole (PPy) and multiwalled carbon nanotubes (MWCNT) were electrochemically synthesized by direct oxidation of pyrrole in 0.1 M aqueous solution of dodecylbenzene sulfonic acid containing a certain amount of MWCNT. The morphology, electronic conductivity, and thermal stability of the composite films have been studied by scanning electron microscopy, Raman spectroscopy and thermal gravimetric analysis. It was found that the mixing sequence of the surfactant, the monomer and MWCNT strongly influenced the compositions and thermal stability of the composite films. Raman spectroscopic studies indicated that the contents of the oxidized species of PPy in the composite films decreased faster than that of the neutral species during the heating process. The conductivity of each composite film showed a maximum in the temperature scale of 120–180 °C and then decreased dramatically with the increase of temperature.

Keywords: Polymers; Carbon nanotubes; Polypyrrole; Raman scattering; Thermal stability; Electrochemistry; Surface structure

1. Introduction

Polypyrrole (PPy), one of the most important conducting polymers, have potential applications in batteries [1,2], supercapacitors [3], sensors [4,5], microwave shielding and corrosion protection [6,7]. In order to increase the physical properties of PPy, various composites of PPy have been synthesized [8–11]. Carbon nanotubes are of interest for composite materials because of their good electronic and mechanical properties and high stability [12–15]. Composites of PPy and carbon nanotubes have been prepared by chemical or electrochemical oxidation, and the capacitance [16,17] and magnetic properties [18] of these composites have also been studied.

In this paper, we report electrochemical synthesis of polypyrrole-multiwalled carbon nanotube (PPy-MWCNT) composite films by direct oxidation of pyrrole in 0.1 M aqueous solution of dodecylbenzene sulfonic acid (DBSA) and containing a certain amount of MWCNT. Especially, the effect of the polymeric solution preparation sequence on the properties of the resulting films were also investigated.

2. Experimental details

2.1. Chemicals

Pyrrole (98%) was purchased from the Chinese Army Medical Institute (Beijing, China) and used after distillation under reduced pressure (~1200 Pa). DBSA was purchased from ACROS (96%) and used without further purification. MWCNT was synthesized in our lab by catalytic pyrolysis of C_3H_6 using Fe as the catalyst. The MWCNT was treated

* Corresponding authors. Tel.: +86 10 6277 3743; fax: +86 10 6277 1149.
E-mail address: gshi@tsinghua.edu.cn (G. Shi).

0040-6090/$ - see front matter © 2004 Elsevier B.V. All rights reserved.
doi:10.1016/j.tsf.2004.08.011

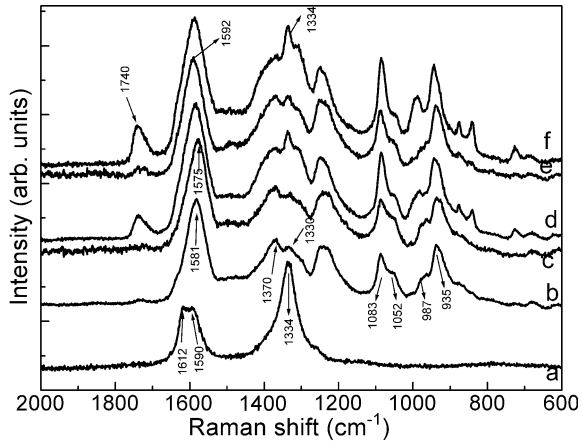

Fig. 1. The Raman spectra of MWCNT, pure PPy and PPy-MWCNT composite films. (a) Pure MWCNT, (b) pure PPy, (c, d) composite films prepared through procedure 2 and (e, f) through procedure 1 with feeding mass ratios of 7 Py/1.5 MWCNT(c, e) and 2 Py/2 MWCNT (d, f).

in hot H_2SO_4–HNO_3 mixed acid (3:1, by volume) for 15 min according to the procedures reported previously [19].

2.2. Electrosynthesis of PPy-based composite films

Electrochemical syntheses and examinations were performed in a one-compartment cell using a potentiostat-galvanostat (EG&G Princeton Applied Research, model 283) under computer control. Stainless steel sheets (AISI 304) with surface areas of 3×1 cm and 3×2 cm were used as the working and counter electrodes, respectively. In all experiments, a saturated calomel electrode (SCE) was employed as the reference electrode. All electrochemical polymerizations were performed at a constant potential of 0.72 V (versus SCE) and the temperature of 15 °C.

The composite films were prepared through two different procedures: In procedure 1, the MWCNT were dispersed in 0.1 M DBSA aqueous solution and sonicated for 1 h. Then, pyrrole in a certain feeding mass ratio to MWCNT was dissolved in this emulsion solution under ultrasonic stirring for 15 min at room temperature. Then, composite films were electrochemically synthesized by electrolyzing this medium. In procedure 2, the MWCNT were dispersed in deionized water and ultrasonic stirring for 1 h, then pyrrole in a certain feeding mass ratio to MWCNT was dissolved in this solution under ultrasonic stirring. Subsequently, DBSA was added into the mixture to form a 0.1 M surfactant solution by sonication for 15 min. Finally, the mixture was electrolyzed to form the composite films. The feeding mass ratios of the monomer and MWCNT were controlled at 7 Py/1.5 MWCNT and 2 Py/2 WMCNT (mg/mg per milliliter). The solutions were degassed by bubbling dry N_2 gas for 10 min prior to polymerization and maintained a N_2 atmosphere during the experiments. As-grown PPy-MWCNT films were washed repeatedly with deionized water and methanol to remove the electrolyte and the monomer and then dried at room temperature under vacuum (~1500 Pa) for 24 h. For comparison, pure PPy was also polymerized by electrolysis of the aqueous solution of 0.1 M DBSA and 0.1 M pyrrole. The film thickness was controlled by the total charges passed in the cell.

2.3. Characterizations

The PPy films (~12 μm) were peeled off from the electrode surfaces into freestanding states with a knife before characterization. The morphology of the films was studied using field-emission scanning electron microscopy (SEM) (JSE-6700F, JEOL) after sputtering with platinum.

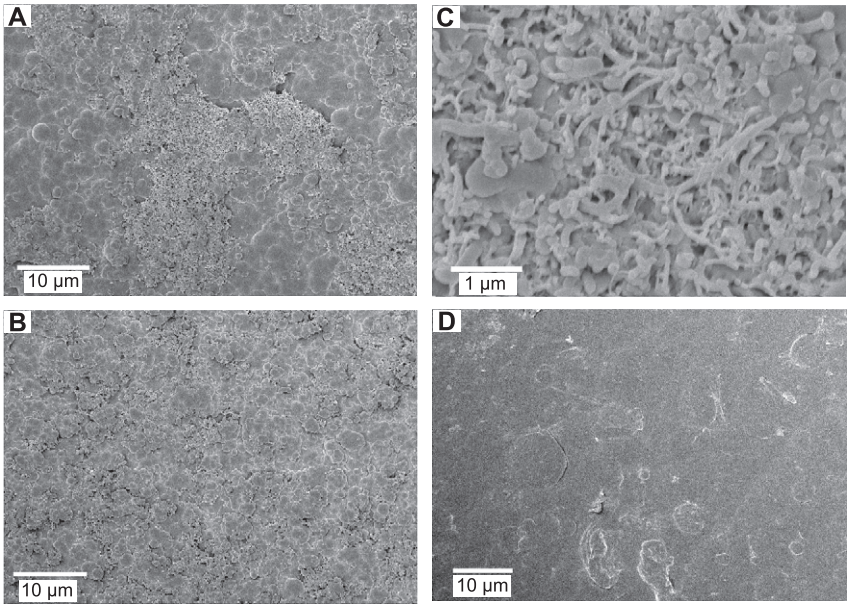

Fig. 2. SEM images of the composite films prepared through procedure 2 (A) and procedure 1 (B, C, in different magnifications) with a feeding ratio of 7 Py/1.5 MWCNT, and pure PPy (D).

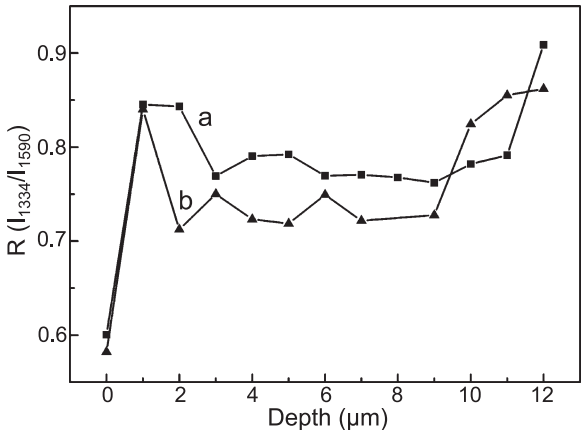

Fig. 3. Depth profile of MWCNT in the sample prepared through procedure 1 (a) and procedure 2 (b) with feeding mass ratio of 2 Py/2 MWCNT.

Raman spectra were recorded on a RM 2000 microscopic confocal Raman spectrometer (Renishaw, England) employing a 633 nm laser beam and a charge coupled device detector with 4 cm^{-1} resolution. The spectra were recorded using a 20× objective and accumulated for 30 s. The power was always kept very low (~0.5 mW) to avoid destroying the samples. The spectra of the PPy films during the heating (heating rate at 5 °C/min, before recording the spectra, the sample was kept at certain temperature for 1 min) were recorded by using a controlled temperature cell set made by Linkam Scientific Instruments. Thermal gravimetric analysis (TGA) were conducted on a Perkin-Elmer TGA-7 under nitrogen protection at a heating rate of 10 °C/min. The dc conductivity during the heating process (15–190 °C) was measured by conventional four-probe method.

3. Results and discussion

3.1. Characterizations of PPy-MWCNT nanocomposites

The Raman spectra of pure PPy, MWCNT, and the PPy-MWCNT composite films are illustrated in Fig. 1. The typical peak of pure MWCNT (Fig. 1a) at 1591 cm^{-1} is attributed to E_{2g} mode of graphite wall [20]. It had also been theoretically deduced that a single-cylinder nanotube should show an E_{2g} mode at 1612 cm^{-1} [21]. The band at 1334 cm^{-1} is assigned to slightly disordered graphite [22]. As can be seen from the spectrum of PPy shown in Fig. 1b, there is a weak C=O band at about 1740 cm^{-1}, indicating that the PPy is slightly overoxidized. The 1581 cm^{-1} band represents the C=C backbone stretching of PPy. The double peaks at about 1052 and 1083 cm^{-1} are assigned to the C–H in plane deformation [23], and another double peak at 1330 and 1370 cm^{-1}, is attributed to the ring-stretching mode of PPy [23,24]. The bands located at about 940 and 990 cm^{-1} are assigned to the ring deformation associated with dication (bipolaron) and radical cation (polaron), respectively [25,26]. The Raman spectra of the composite films showed the bands related to pure PPy and MWCNT (Fig. 1c–f). Furthermore, the intensity of band located at 1334 cm^{-1} increases with the increase of the feeding mass ratio of MWCNT to pyrrole, implying the increase of MWCNT content of the composite film.

Fig. 2 shows the SEM images of pure PPy and its composite films. As can be seen from this figure, the pure PPy film exhibits a smooth surface (Fig. 2D). On the other hand, the surfaces of composite films (Fig. 2A–C) were much rougher than that of pure PPy film. The carbon nanotubes coated with PPy together with the particles of pure PPy formed the surfaces of the composite films (Fig. 2C). According to a previous study [27], surfactant molecules could be adsorbed strongly onto the MWCNT surface through van der Waals' force and form sheaths around the tubes, which made the nanotubes disperse in the solution uniformly and stably. As a result, MWCNTs are more uniformly dispersed in the composite film prepared by mixing MWCNT with aqueous DBSA solution firstly (procedure 1, see Experimental details) (Fig. 2B) than that in the film synthesized by mixing MWCNT with deionized water first (procedure 2) (Fig. 2A).

In order to evaluate the relative contents of MWCNT in different depths of the composite films, the composite film

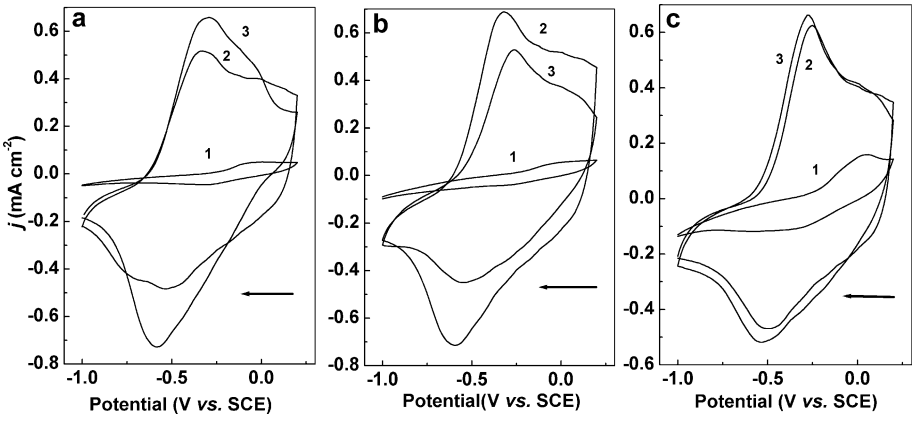

Fig. 4. Cyclic voltammograms of the as-grown PPy polymer films in the aqueous solution of 0.1 M TBABr (1), $LiClO_4$ (2) or NaDBSA (3). (a) Pure PPy, (b) composite film prepared through procedure 1 and (c) through procedure 2 with feeding mass ratio of 2 Py/2 MWCNT. Potential scan rate 20 mV s^{-1}.

was cut vertically into two pieces and the laser light spot was focused on the newly formed cross-section to record the Raman spectra. The plot of the intensity ratio of 1334 and 1590 cm^{-1} bands (I_{1334}/I_{1590}) versus depth profile of composite film prepared from electrolytes with mass feeding ratio of 2 Py/2 MWCNT is demonstrated in Fig. 3. The position at 0 μm corresponded to the surface of the composite film in contact with the electrode surface and the position of 12 μm reflected the surface of the film in contact with the electrolyte solution. From this figure, we found that the composite film contained less MWCNT at the beginning stage of electropolymerization. The surface of the film contained more nanotubes than that in the bulk film.

The electroactivity of the pure (a) and the composite PPy films (b, c) described above deposited for 200 mC cm^{-2} were studied in a monomer-free 0.1 M aqueous solution of tetrabutylammonium bromide (TBABr) (1), $LiClO_4$ (2), or NaDBS (3), respectively (Fig. 4). As can be seen from this figure, each of the CVs shows a couple of broad cathodic and anodic peaks. In the solution of $LiClO_4$ and NaDBS, the cathodic peak was found at about −0.5 to −0.6 V and the anodic peak was at about −0.3 V, indicating the insertion and expulsion of small cation ions of Li^+ or Na^+ [28,29]. However, in the solution of TBABr, there are very weak cathodic and anodic responses in comparison to those shown in Fig. 4A and B, mainly due to that the larger size of $N^+(CH_3CH_2CH_2CH_2)_4$ ions disable the cation to be involved in the ion exchange. There is no significant difference between the CVs of pure PPy and PPy-MWCNT, indicating that the electrochemical activity of the composite film results from its PPy component.

3.2. Investigations of thermal stability of the composite films

Fig. 5 shows the TGA curves of MWCNT, pure PPy and composite films in a nitrogen atmosphere. MWCNT were stable and did not show dramatic decomposition in the temperature range of 25–900 °C, and 66% mass was reserved at 900 °C (Fig. 5f). Pure PPy films are stable in the temperature range of 25–240 °C, and showed only ca. 5% mass loss. However, a rapid mass loss occurred in the range of 240–900 °C, and only 13% mass remained for pure PPy at 900 °C (Fig. 5a). Otherwise, more mass remained for composite films of PPy-MWCNT than pure PPy at 900 °C (Fig. 5b–e).

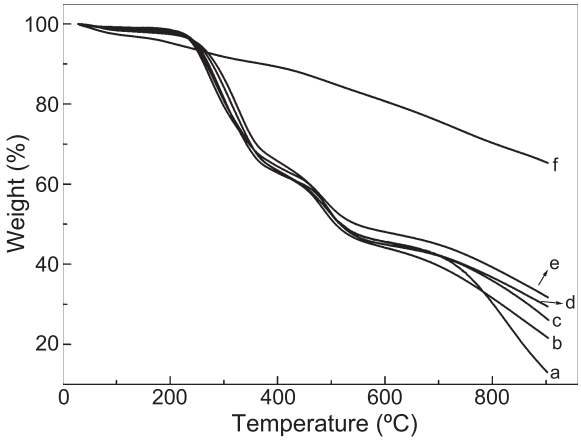

Fig. 5. Thermal gravimetric analysis of pure PPy (a) and composite films prepared through procedure 2 (b, d) and procedure 1 (c, e) with feeding ratio of 7 Py/1.5 MWCNT (b, c) and 2 Py/2 MWCNT (d, e), and MWCNT (f).

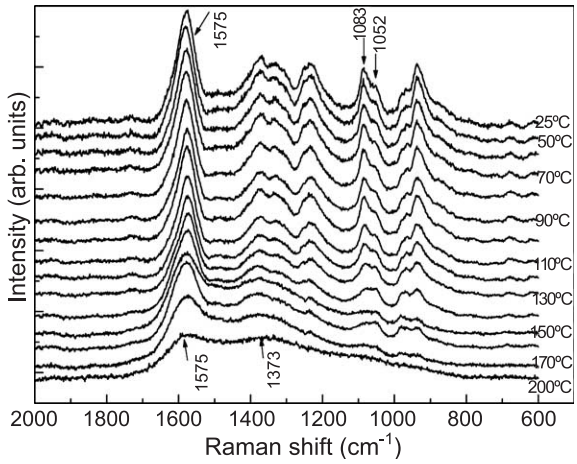

Fig. 6. Raman spectra of the composite film prepared through procedure 2 with feeding mass ratio of 7 Py/1.5 MWCNT at different temperatures recorded during the heating process.

In the Raman spectra of PPy, the bands at 1083 and 1370 cm^{-1} belong to the C–H in-plane and ring stretching, respectively, are assigned to the oxidized species of PPy according to the literature [25,26]. The conductivity of the PPy is strongly related to the intensities of these two bands. The Raman spectra of the sample prepared through procedure 2 (7 Py/1.5 MWCNT), recorded during the heating process, are illustrated in Fig. 6. The spectrum of as-grown PPy film at room temperature shows strong Raman bands related to the oxidized and neutral species. The Raman bands related to the oxidized and neutral species decrease with the increase of temperature. However, the decrease rates of the Raman bands related to the oxidized

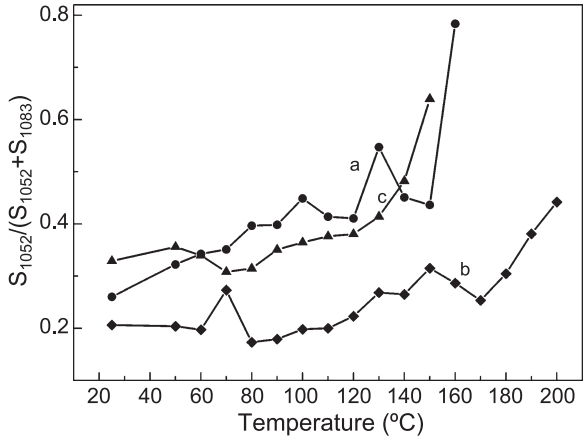

Fig. 7. The plots of the ratios of $S_{1052}/(S_{1052}+S_{1083})$ versus temperature. (a) Pure PPy and composite films prepared through procedure 1 (b) and procedure 2 (c) with feeding mass ratio of 7 Py/1.5 MWCNT.

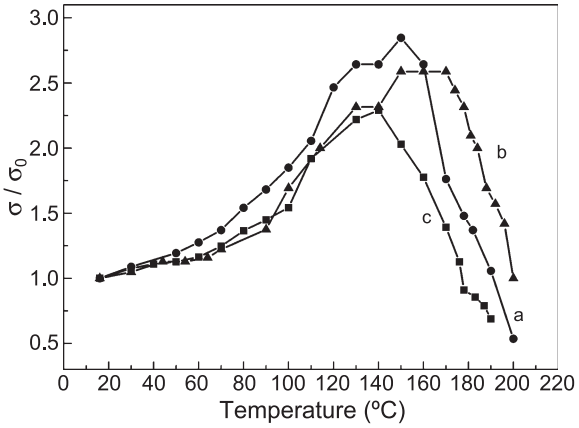

Fig. 8. The plots of dc conductivity ratios of σ/σ_0 versus temperature during the heating process. (a) Pure PPy, (b) and (c) are composite films prepared through procedures 1 and 2 with feeding mass ratio of 7 Py/1.5 MWCNT, respectively.

species is faster than those of the bands associated with the neutral species. Finally, the PPy sample was decomposed and showed a spectrum with features similar to that of a carbonaceous material at about 200 °C. Two broad bands appeared at about 1575 and 1373 cm^{-1}, respectively [30]. The other PPy-MWCNT and pure PPy films showed similar spectral phenomena.

In order to illustrate the changes of the PPy films during the heating process, the broad Raman peaks of PPy appeared in the range of 1015–1145 cm^{-1} were further divided into their individual component peaks which are located at 1052 cm^{-1} and 1083 cm^{-1} by using an "automatic fitting" program provided by the Raman spectrometer. The plots of the band area ratios of the band related to the neutral species and the area sum of the band related to the oxide and neutral species of neutral species ($R=S_{1052}/(S_{1052}+S_{1083})$) versus temperature is demonstrated in Fig. 7. As can be seen from this figure that the thermal stabilities of the PPy composite films are different. The film prepared through procedure 1 was thermally more stable than the sample prepared through procedure 2 and pure PPy. The film prepared through procedure 2 has the lowest thermal stability. This indicates that the carbon nanotubes can increase or decrease the thermal stability of PPy films in composite to pure PPy film, based on the mixing sequence of carbon nanotubes with DBSA and pyrrole.

The conductivities of pure PPy and composite films prepared through procedures 1 and 2 (7 Py/1.5 MWCNT) were measured to be 22.3, 17.2 and 26.0 S cm^{-1}, respectively. The temperature dependence of conductivity was measured in the scale of 16–200 °C, and plotted in Fig. 8. As can be seen from this figure, the conductivities of the films increase with the temperature increase initially due to the semiconductor property of the polymers [18,31]. After reaching a maximum in the temperature scale of 120–180 °C, the conductivities decreased dramatically because the structures of the polymers were decomposed by heating.

From this figure, we can also see that the composite films have different thermal stabilities. The thermal stability of sample prepared through procedure 1 was the highest and prepared through procedure 2 (7 Py/1.5 MWCNT) was the lowest among the three films. After heating at 190 °C for 2 min, the sample was cooled slowly to 15 °C. We found the conductivity of pure PPy, samples prepared through procedures 1 and 2 remained at 42%, 74% and 16.5%, respectively. These results indicated that the carbon nanotubes mixed with DBSA firstly favored to form composite films with higher thermal stability. Otherwise, when carbon nanotubes mixed with pyrrole firstly, the composite exhibit lower thermal stability than that of pure PPy.

4. Conclusions

The PPy-MWCNT composite films can be synthesized electrochemically. Heating the PPy samples leads to the destruction of the oxidized species of the polymer, and finally, the polymer decomposed into a carbonaceous material. The MWCNT can increase the thermal stability of PPy when the MWCNT mixed with DBSA firstly. In this case, the nanotubes dispersed in the films uniformly. Otherwise, MWCNT decrease the thermal stability of the PPy when carbon nanotubes mixed with pyrrole firstly because the pyrrole could not disperse the nanotubes uniformly.

Acknowledgements

This work was supported by National Natural Science Foundation of China with grant numbers 50225311, 20374034 and 50133010.

References

[1] J.H. Chen, Z.P. Huang, D.Z. Wang, S.X. Yang, W.Z. Li, J.G. Wen, Z.F. Ren, Synth. Met. 125 (2001) 289.
[2] J.U. Kim, I.S. Jeong, S.I. Moon, H.B. Gu, J. Power Sources 97/98 (2001) 450.
[3] K. Jurewicz, S. Delpeux, V. Bertagna, F. Beguin, E. Frackowiak, Chem. Phys. Lett. 347 (2001) 36.
[4] C.W. Lin, B.J. Hwang, C.R. Lee, Mater. Chem. Phys. 55 (1998) 139.
[5] M. Hepel, J. Electrochem. Soc. 145 (1998) 124.
[6] V.T. Truong, P.K. Lai, B.T. Moore, R.F. Muscat, M.S. Russo, Synth. Met. 110 (2000) 7.
[7] L.J. Buckley, M. Eashoo, Synth. Met. 78 (1996) 1.
[8] P. Zhang, D.J. Wang, S.H. Kan, X.D. Chai, J.Z. Liu, T.J. Li, Z.H. Yang, Synth. Met. 84 (1997) 165.
[9] Y.C. Liu, C.J. Tsai, J. Electroanal. Chem. 537 (2002) 165.
[10] S. Sinharay, M. Biswas, Mater. Res. Bull. 34 (1999) 1187.
[11] Y.C. Liu, C.J. Tsai, Chem. Mater. 15 (2003) 320.
[12] S. Iijima, Nature 354 (1991) 56.
[13] M.R. Falvo, G.J. Clary, R.M. Taylor, V. Chi, F.P. Brooks, S. Washburn, R. Superfine, Nature 389 (1997) 582.
[14] M.M.J. Treacy, T.W. Ebbesen, J.M Gibson, Nature 381 (1996) 678.

[15] C.M. Niu, E.K. Sichel, R. Hoch, D. Moy, H. Tennent, Appl. Phys. Lett. 70 (1997) 1480.
[16] M. Hughes, G.Z. Chen, M.S.P. Shaffer, D.J. Fray, A.H. Windle, Chem. Mater. 14 (2002) 1610.
[17] Q.F. Xiao, X. Zhou, Electrochim. Acta 48 (2003) 575.
[18] J.H. Fan, M.X. Wan, D.B. Zhu, B.H. Chang, Z.W. Pan, S.S. Xe, J. Appl. Polym. Sci. 74 (1999) 2605.
[19] M.S.P. Shaffer, X. Fan, A.H. Windle, Carbon 36 (1998) 1603.
[20] H. Hlura, T.W. Ebbesen, T. Tanigaki, H. Takahashi, Chem. Phys. Lett. 202 (1993) 509.
[21] R.A. Jishi, L. Venkataran, M.S. Dresselhaus, G. Dresselbaus, Chem. Phys. Lett. 209 (1993) 77.
[22] W.A. Deheer, W.S. Bacsa, A. Chatelain, T. Gerfin, R. Humphrey-baker, L. Forro, D. Ugarte, Science 268 (1995) 845.
[23] Y.C. Liu, B.J. Hwang, Synth. Met. 113 (2000) 203.
[24] Y.C. Liu, B.J. Hwang, W.J. Jian, R. Santhanam, Thin Solid Films 374 (2000) 85.
[25] J. Duchet, R. Legras, S. Demoustier-Champagne, Synth. Met. 98 (1998) 113.
[26] A.B. Goncalves, A.S. Mangrich, A.J.G. Zarbin, Synth. Met. 114 (2000) 119.
[27] M.F. Islam, E. Rojas, D.M. Bergey, A.T. Johnson, A.G. Yodh, Nano Lett. 3 (2003) 269.
[28] M.R. Gandhi, P. Murray, G.M. Spinks, G.G. Wallace, Synth. Met. 73 (1995) 247.
[29] J.M. Davecy, S.F. Ralph, C.O. Too, G.G. Wallace, Synth. Met. 99 (1999) 191.
[30] G.Q. Shi, F.G. Chen, S.X. Wu, Y.F. Zhu, X.Y. Hong, W.H. Hou, L. Ming, J. Appl. Polym. Sci. 81 (2001) 116.
[31] P. Fedorko, V. Skakalova, Synth. Met. 94 (1998) 279.